



**Repositorio Institucional de la Universidad Autónoma de Madrid**

<https://repositorio.uam.es>

Esta es la **versión de autor** de la comunicación de congreso publicada en:  
This is an **author produced version** of a paper published in:

IEEE 2nd. International Conference on Biometrics: Theory, Applications  
and Systems (BTAS). IEEE, 2008. 1-6

**DOI:** <http://dx.doi.org/10.1109/BTAS.2008.4699329>

**Copyright:** © 2008 IEEE

El acceso a la versión del editor puede requerir la suscripción del recurso  
Access to the published version may require subscription

# On the Effects of Time Variability in Iris Recognition

P. Tome-Gonzalez, F. Alonso-Fernandez and J. Ortega-Garcia

**Abstract**—In this paper, we evaluate the effects of time separation between acquisitions in iris recognition. We use for our experiments a publicly available iris recognition system and the BiosecuID database, containing 8128 iris images of 254 individuals acquired in four acquisition sessions, separated by one to four weeks between consecutive sessions. Reported results show that time separation between iris samples under comparison has severe impact on the recognition rates. An important degradation on the False Rejection Rate is observed, meaning that the intra-class variability is increased. All images in our database have been acquired under similar controlled conditions and with the same sensor.

**Index Terms**—Biometrics, image processing, pattern recognition, iris recognition, time separation

## I. INTRODUCTION

Biometric authentication has been receiving a considerable attention over the last years due to the increasing demand for automatic person recognition. The term *biometrics* refers to automatic recognition of an individual based on anatomical (e.g., fingerprint, face, iris, hand geometry, ear, palmprint) or behavioral characteristics (e.g., signature, gait, keystroke dynamics), which cannot be stolen, lost or copied [1]. Among all biometric techniques, iris recognition has been traditionally regarded as one of the most reliable and accurate biometric identification system available [2].

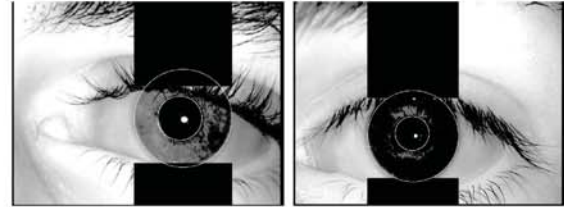
One of the drawbacks of a biometric system is the variability in the acquired data. The biometric data acquired from an individual during authentication may be very different from the data that was used to generate the template during enrollment, thereby affecting the matching process [1]. In this paper, we evaluate the effects of time separation between acquisitions in iris recognition. Our goal is to determine to what extent recognition rates are degraded when time between sample acquisition is increased. Experiments reported here show that the False Rejection Rate is dramatically worsened. Subsequent experiments suggest that this degradation in the error rates is not caused by variations in the user-sensor interaction, but by a reduction in the similarity between iris templates across time.

## II. RECOGNITION SYSTEM

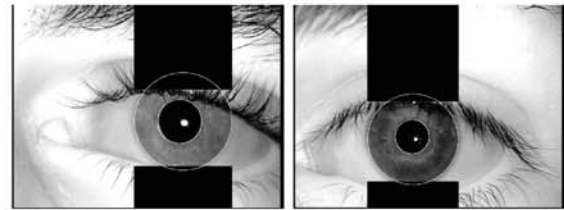
We have used for our experiments the iris recognition system<sup>1</sup> developed by Libor Masek [3], [4]. It consists of the following sequence of steps that are described next: segmentation, normalization, encoding and matching.

Biometric Recognition Group - ATVS, Escuela Politecnica Superior, Universidad Autonoma de Madrid, Avda. Francisco Tomas y Valiente, 11, Campus de Cantoblanco, 28049 Madrid, Spain, email: {pedro.tome, fernando.alonso, javier.ortega}@uam.es

<sup>1</sup>The source code can be freely downloaded from [www.csse.uwa.edu.au/~pk/studentprojects/libor/sourcecode.html](http://www.csse.uwa.edu.au/~pk/studentprojects/libor/sourcecode.html)

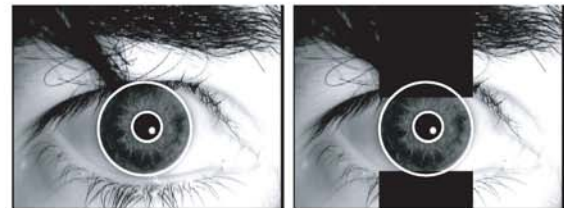


(a) Using detection of eyelashes



(b) Not using detection of eyelashes

Fig. 1. Example of eyelids and eyelashes removal.



(a) Original image and noise image



(b) Template of image



(c) Noise mask

Fig. 2. Example of the normalization step.

### A. Segmentation and Normalization

For the iris segmentation task, the system uses circular Hough transform in order to detect the iris and pupil boundaries. Iris boundaries are modeled as two concentric circles. The range of search radius values is set manually. A maximum value is also imposed to the distance between the circle's center. An eyelids and eyelashes removal step is also performed in the system. Eyelids are isolated first by fitting a line to the upper and lower eyelid using the linear Hough transform. Eyelashes isolation is then performed by histogram thresholding. An example can be seen in Figure 1.



For normalization of iris regions, a technique based on Daugman's rubber sheet model is employed. The centre of the pupil is considered as the reference point, and radial vectors pass through the iris region. Since the pupil can be non-concentric to the iris, a remapping formula for rescale points depending on the angle around the circle is used. Normalization produces a 2D array with horizontal dimensions of angular resolution and vertical dimensions of radial resolution, in addition to another 2D noise mask array for marking reflections, eyelashes, and eyelids detected in the segmentation stage. In Figure 2, an example of the normalization step is depicted.

### B. Feature encoding and Matching

Feature encoding is implemented by convolving the normalized iris pattern with 1D Log-Gabor wavelets. The 2D normalized pattern is broken up into a number of 1D signals, and then these 1D signals are convolved with 1D Gabor wavelets. The rows of the 2D normalized pattern are taken as the 1D signal, each row corresponds to a circular ring on the iris region. It uses the angular direction since maximum independence occurs in this direction [3].

The output of filtering is then phase quantized to four levels using the Daugman method [5], with each filtering producing two bits of data. The output of phase quantization is a grey code, so that when going from one quadrant to another, only 1 bit changes. This will minimize the number of bits disagreeing, if say two intra-class patterns are slightly misaligned and thus will provide more accurate recognition [3]. The encoding process produces a bitwise template containing a number of bits of information, and a corresponding noise mask which represents corrupt areas within the iris pattern.

For matching, the Hamming distance (HD) is chosen as a metric for recognition, since bitwise comparisons are necessary. The Hamming distance employed incorporates noise masking, so that only significant bits are used in calculating the Hamming distance between two iris templates. The modified Hamming distance formula is given by

$$HD = \frac{\sum_{j=1}^N X_j (\text{XOR}) Y_j (\text{AND}) Xn'_j (\text{AND}) Yn'_j}{N - \sum_{k=1}^N Xn_k (\text{OR}) Yn_k} \quad (1)$$

where  $X_j$  and  $Y_j$  are the two bitwise templates to compare,  $Xn_j$  and  $Yn_j$  are the corresponding noise masks for  $X_j$  and  $Y_j$ , and  $N$  is the number of bits represented by each template.

In order to account for rotational inconsistencies, when the Hamming distance of two templates is calculated, one template is shifted left and right bitwise and a number of Hamming distance values is calculated from successive shifts [5]. This method corrects for misalignments in the normalized iris pattern caused by rotational differences during imaging. From the calculated distance values, the lowest one is taken.



Fig. 3. LG Iris Access 3000 sensor.

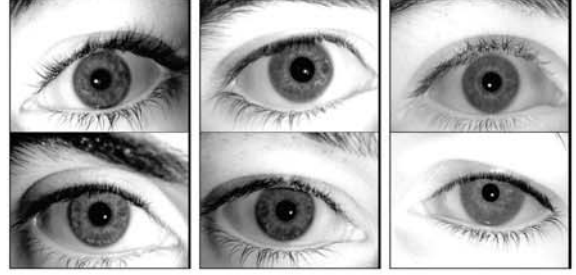


Fig. 4. Iris examples from the BioSecurID database.

## III. EXPERIMENTS

### A. Database and Protocol

For the experiments in this paper, we use the BioSec baseline [6] and BioSecurID [7] databases. The BioSec database consists of 200 individuals acquired in two acquisition sessions, separated typically by one to four weeks. The BioSecurID database is formed 254 individuals acquired in four acquisition sessions, separated typically by one to four weeks between consecutive sessions. A total of four iris images of each eye, changing eyes between consecutive acquisitions, are acquired in each session for both databases. The total number of iris images is therefore: 200 individuals  $\times$  2 sessions  $\times$  2 eyes  $\times$  4 iris = 3200 iris images for the BioSec baseline database, and 254 individuals  $\times$  4 sessions  $\times$  2 eyes  $\times$  4 iris = 8128 iris images for the BioSecurID database. We consider each eye as a different user, thus

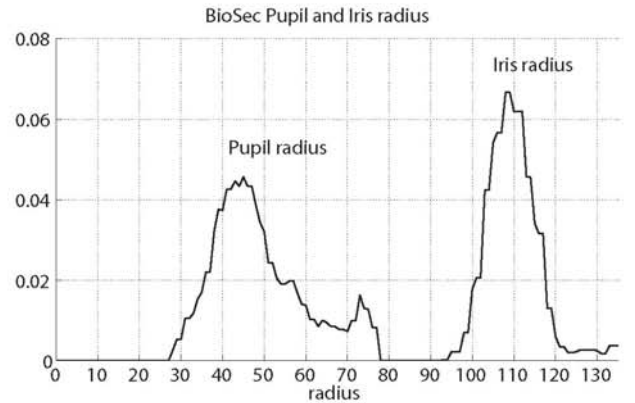


Fig. 5. Distribution of radii of the BioSec database.

having 400 users in the Biosec database and 508 users in the BioSecurID database. Glasses were removed for the acquisition, while the use of contact lenses was allowed.

Both databases used the same LG Iris Access 3000 sensor, with an image size of 640 pixels width and 480 pixels height (see Figure 3). This sensor incorporates a built-in quality checking process: a sequence of 20 images is acquired and the best of them is selected. Previous to this sequence acquisition, the camera automatically checks subject's positioning and distance to ensure proper focus (if this checking fails, no sequence is acquired). Specular reflection is positioned in the pupil region (outside of the iris region, see Figure 4 for example) due to the proper positioning of a set of LED-based light sources. Acquisition of the databases was done in an office-like environment under the supervision of a human operator that gave the necessary instructions and guidance. Regarding the environmental conditions, neutral lighting with no preponderant focuses was used, and the pose of the contributor was frontal while sitting in a non-revolving chair.

The Biosec database is used here to tune the parameters of the verification system, namely the range of radii of circles modeling iris boundaries, as well as the maximum distance allowed between the centers of both circles. Once tuned the system, the BioSecurID database is used for testing. In Figure 4, some iris samples from the BioSecurID subcorpus are shown. Eyelashes detection is not performed in our experiments. Although eyelashes are quite dark compared with the surrounding iris region, other iris areas are equally dark due to the imaging conditions. Therefore, thresholding to isolate eyelashes would also remove important iris regions, as shown in Figure 1, making this technique infeasible. However, eyelash occlusion is not very prominent in our databases, so no technique was implemented to isolate eyelashes.

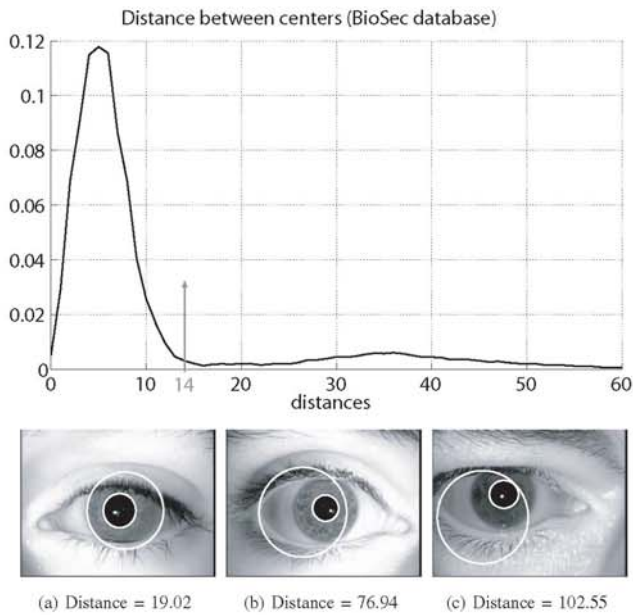


Fig. 6. Distribution of distance between centers of pupil and iris circumferences (top) and examples of images that fails extraction (bottom).

Database		Number of valid images	% of success
BioSec	Session 1	1301	81.31%
	Session 2	1330	83.12%
	Total	2631	82.21%
BioSecurID	Session 1	1560	76.77%
	Session 2	1557	76.62%
	Session 3	1554	76.47%
	Session 4	1552	76.37%
	Total	6223	76.56%

TABLE I

VALID IMAGES CORRECTLY SEGMENTED FOR EACH DATABASE.

#### Intra-session matches

	USER	IMPOSTOR
Session 1	2036	1213984
Session 2	2019	1209327
Session 3	2015	1204666
Session 4	2007	1201569

#### Inter-session matches

	USER	IMPOSTOR
Session 1 vs. Session 2	5310	219981
Session 1 vs. Session 3	5316	218573
Session 1 vs. Session 4	5319	221377

TABLE II

NUMBER OF AVAILABLE MATCHES IN THE EXPERIMENTS.

For evaluation of the verification performance, the following experiments are carried out in the BioSecurID database: *i*) matching between iris of the same session (*intra-session* evaluation); and *ii*) matching between iris of the first session against each of the others sessions (*inter-session* evaluation). For the *intra-session* evaluation, the experimental protocol is as follows. Genuine matches are obtained by comparing each of the four images of a user to the remaining images of the same user, but avoiding symmetric matches. Impostor matches are obtained by comparing the first image of a user to the four iris images of the remaining users, avoiding symmetric matches. This process is repeated for the four different sessions, resulting on four sets of scores, one per session. For the *inter-session* evaluation, the experimental protocol is as follows. For a given user, all the images of the first session are considered as enrolment templates. Genuine matches are obtained by comparing the templates to the corresponding images of the second (third, fourth) session from the same user. Impostor matches are obtained by comparing one randomly selected template of a user to a randomly selected iris image of the second (third, fourth) session from the remaining users. As a result, three sets of scores are obtained.

#### B. Results and discussion

In Figure 5 we plot the distribution of radii of circles modeling iris boundaries for the Biosec database. Based on this histogram, we set a range from 90 to 130 pixels for the outer circle and 28 to 78 pixels for the inner circle. It is also depicted in Figure 6 the distribution of distance between



centers of pupil and iris circumferences (top) and examples of images that fails extraction (bottom) when a threshold value of 14 is set. With these constraints, for the BioSec database we obtain 2631 iris images correctly extracted of the 3200 iris images available, which corresponds to a success rate of around 82.32%. For BioSecurID, we get 6223 iris images correctly extracted of the 8128 iris images available, which corresponds to a success rate of around 76.56%. These figures are summarized in Table I. They are consistent with those of [3], where a success rate of around 83% was reported on the CASIA database using the same system. As a result, it is not possible to use all the eye images from the BioSecurID database for testing experiments. The number of available matches are summarized in Table II.

Verification results for the intra- and inter-session experiments are reported in Table III. FRR at three specific FAR points is reported. In Figure 7, distributions of FR and FA errors are also depicted. It is observed that error rates are increased considerably in the *inter-session* experiments with respect to the *intra-session* ones (an increase of more than twice as many is observed). This reveals that time separation between samples being compared has impact on the recognition rates. From Figure 7, it is worth noting that degradation occurs on the FRR, not on the FAR, meaning that the system remains enough robust to impostor accesses across time but that intra-class variability is increased. These results are mirrored in Table IV, where the mean and standard deviation values of genuine and impostor score distributions are given, together with a plot of their distributions. Interestingly enough, we observe that only the mean value of genuine score distributions is affected, but not its standard deviation. We also give in Table IV the Fisher Distance between genuine and impostor score distributions, which is defined as [8]:

$$FD = \frac{(\mu_G - \mu_I)^2}{\sigma_G^2 + \sigma_I^2} \quad (2)$$

where  $\mu_G$  and  $\sigma_G$  ( $\mu_I$  and  $\sigma_I$ ) are the mean and variance of the genuine score distribution (impostor score distribution). A significant reduction is observed in the FD for the inter-session experiments with respect to the intra-session ones.

By looking at the intra-session experiments of Table III, no general trend can be observed in the error rates among different sessions. This can also be observed in the score distributions of Table IV (top). On the other hand, we observe from the inter-session experiments that as time separation between samples is increased, higher error rates are obtained. Particularly, clear differences are observed between the “s1-s2” line of Figure 7 and the other ones. It seems, however, that once that a minimum time between samples has passed, error rates are not apparently increased. This is observed in Figure 7, where an small separation between lines marked “s1-s3” and “s1-s4” can be seen.

We now study the differences observed in the genuine score distributions between intra- and inter-class experiments. We plot in Figure 8 the distribution of the two terms

FRR - INTRA-SESSION EXPERIMENTS

	Session 1	Session 2	Session 3	Session 4
<b>FAR=0.01</b>	9.8723	8.469	10.074	11.2606
<b>FAR=0.1</b>	6.9008	6.835	7.593	7.2995
<b>FAR=1</b>	5.2063	5.0220	5.4839	5.3812

FRR - INTER-SESSION EXPERIMENTS

	S1 versus S2	S1 versus S3	S1 versus S4
<b>FAR=0.01</b>	22.429	25.809	24.262
<b>FAR=0.1</b>	16.7797	18.764	18.227
<b>FAR=1</b>	11.4783	13.497	14.0158

TABLE III

RESULTS FOR THE INTRA-SESSION AND INTER-SESSION EXPERIMENTS.

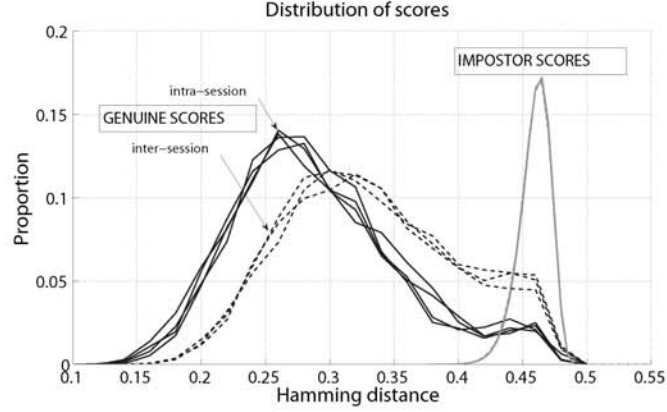
FRR AT THREE SPECIFIC FAR POINTS IS REPORTED (IN %).

of the Hamming distance (Equation 1): the denominator (left part of Figure 8) accounts for the number of significant bits between the two bitwise templates under comparison, whereas the numerator (right part of Figure 8) is the number of dissimilar bits between them. It is clearly observed that when time separation is allowed, the number of dissimilar bits between the samples is increased. In other words, the similarity between two iris templates is reduced if they are acquired at different moments (in our experiments, the minimum separation is one to four weeks between any two consecutive sessions). However, as observed before, once that a minimum time between samples has passed, the similarity is not reduced anymore.

The databases used in our experiments have been acquired under supervision of an operator, with neutral lighting and frontal pose of the contributor. As a result, no significant differences are expected between iris images of different sessions due to the acquisition process. This is consistent with Figure 8 (left), where the number of significant bits between iris templates remains constant with time. We also plot in Figure 9 the distribution of several geometrical parameters of the BioSecurID database, namely: radius of the pupil and iris, area of the iris, and size of the noise mask. No remarkable differences are found in these parameters for the different sessions, thus suggesting that the acquisition process itself has not impact on the differences observed above in the error rates.

#### IV. CONCLUSIONS

The effects of time separation between samples acquisition in iris recognition is studied. A publicly available iris recognition system and the BioSecurID database are used in our experiments. This database contains iris images of 254 individuals acquired in four acquisition sessions, separated by one to four weeks between consecutive sessions, thus allowing to evaluate time variability. We observe that time separation between iris samples being compared has impact on the recognition rates. An increase of more than twice as many is observed in the False Rejection Rate. On the contrary, no effect is observed in the False Acceptance Rate.



INTRA-SESSION EXPERIMENTS						INTER-SESSION EXPERIMENTS					
	$\mu_G$	$\sigma_G$	$\mu_I$	$\sigma_I$	FD		$\mu_G$	$\sigma_G$	$\mu_I$	$\sigma_I$	FD
<b>Session 1</b>	0.29	0.067	0.46	0.012	6.11	<b>S1-S2</b>	0.33	0.067	0.46	0.013	3.62
<b>Session 2</b>	0.29	0.064	0.46	0.012	6.63	<b>S1-S3</b>	0.34	0.068	0.46	0.013	3.24
<b>Session 3</b>	0.29	0.068	0.46	0.012	6.07	<b>S1-S4</b>	0.34	0.068	0.46	0.013	3.24
<b>Session 4</b>	0.30	0.066	0.46	0.013	6.05						

TABLE IV

RESULTS FOR THE INTRA-SESSION AND INTER-SESSION EXPERIMENTS. FISHER DISTANCE (FD) BETWEEN GENUINE AND IMPOSTOR SCORE DISTRIBUTIONS IS GIVEN. MEAN AND STANDARD DEVIATION OF GENUINE (IMPOSTOR) SCORE DISTRIBUTIONS ARE DENOTED AS  $\mu_G$  AND  $\sigma_G$  ( $\mu_I$  AND  $\sigma_I$ ) RESPECTIVELY.

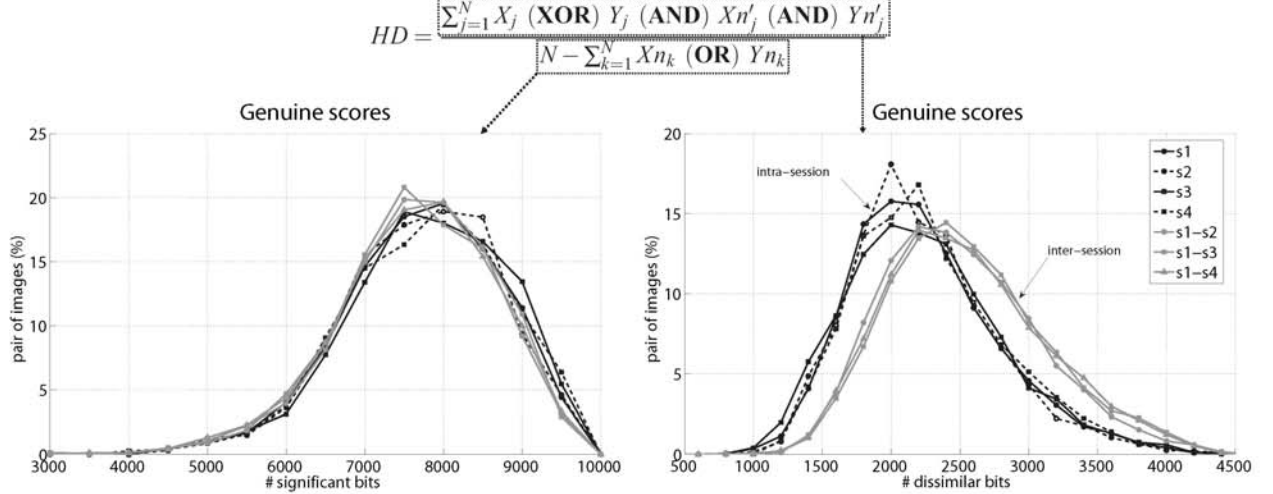


Fig. 8. Genuine scores. Distribution of the two terms of the Hamming distance (Equation 1) for the intra-session and inter-session experiments..

This means that the system remains enough robust to impostor accesses across time but that intra-class variability is increased. A subsequent analysis suggest that this difference in performance across time is not caused by the acquisition process (i.e. different interaction with the sensor) but by a reduction of similarity between iris template across time.

Existing technology evaluations have not taken into account the effects of timing in iris recognition [9]. Results of this paper motivates us to conduct further experiments using

other recognition algorithms and acquisition devices [10]. Also, to cope with this problem, template update techniques, the use of multiple templates [11] and the incorporation of quality measures [12] are being studied.

## V. ACKNOWLEDGMENTS

This work has been supported by Spanish MCYT TEC2006-13141-C03-03 project. Author F. A.-F. thanks Consejería de Educacion de la Comunidad de Madrid and



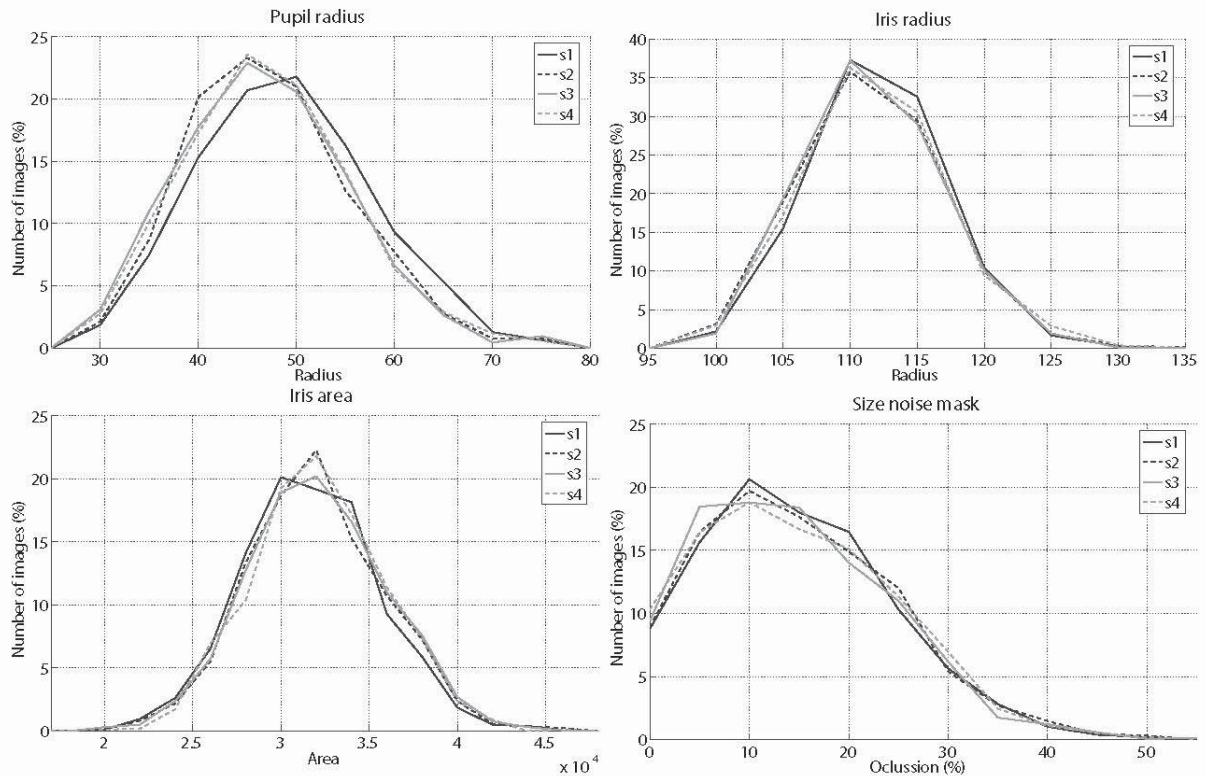


Fig. 9. Distribution of several geometrical parameters of the four sessions (s1 to s4) of the BiosecuID database.

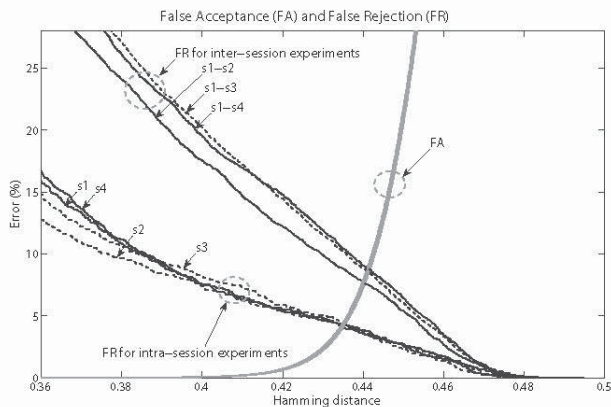


Fig. 7. FA and FR for the intra-session and inter-session experiments.

Fondo Social Europeo for supporting his PhD studies.

#### REFERENCES

- [1] A. Jain, A. Ross, and S. Pankanti, "Biometrics: A tool for information security," *IEEE Trans. on Information Forensics and Security*, vol. 1, pp. 125–143, 2006.
- [2] A. Jain, R. Bolle, and S. Pankanti, Eds., *Biometrics - Personal Identification in Networked Society*. Kluwer Academic Publishers, 1999.
- [3] L. Masek, "Recognition of human iris patterns for biometric identification," Ph.D. dissertation, Technical Report, The school of Computer Science and Software Engineering, The University of Western Australia, 2003.
- [4] L. Masek and P. Kovesi, "Matlab source code for a biometric identification system based on iris patterns," *The School of Computer Science and Software Engineering, The University of Western Australia*, 2003.
- [5] J. Daugman, "How iris recognition works," *Proceedings of 2002 International Conference on Image Processing*, vol. 1, pp. 22–25, 2002.
- [6] J. Fierrez, J. Ortega-Garcia, D. Torre-Toledano, and J. Gonzalez-Rodriguez, "BioSec baseline corpus: A multimodal biometric database," *Pattern Recognition*, vol. 40, no. 4, pp. 1389–1392, April 2007.
- [7] J. Galbally, J. Fierrez, J. Ortega-Garcia, M. Freire, F. Alonso-Fernandez, J. Siguenza, J. Garrido-Salas, E. Anguiano-Rey, G. Gonzalez-de-Rivera, R. Ribalda, M. Faundez-Zanuy, J. Ortega, V. Cardeoso-Payo, A. Viloria, C. Vivaracho, Q. Moro, J. Igarza, J. Sanchez, I. Hernaez, and C. Orrite-Uruela, "BiosecuID: a Multimodal Biometric Database," *Proc. MADRINET Workshop*, pp. 68–76, November 2007.
- [8] G. Marcialis and F. Roli, "Fusion of multiple fingerprint matchers by single-layer perceptron with class-separation loss function," *Pattern Recognition Letters*, vol. 26, pp. 1830–1839, 2005.
- [9] E. Newton and P. Phillips, "Meta-analysis of third party evaluations of iris recognition," *NISTIR 7440*, 2007.
- [10] K.W. Bowyer, K. Hollingsworth, and P. Flynn, "Image understanding for iris biometrics: a survey," *Computer Vision and Image Understanding*, vol. 110, pp. 281–307, 2008.
- [11] U. Uludag, A. Ross, and A. Jain, "Biometric template selection and update: a case study in fingerprints," *Pattern Recognition*, vol. 37, pp. 1533–1542, 2004.
- [12] Y. Chen, S. Dass, and A. Jain, "Localized iris image quality using 2-D wavelets," *Proc. International Conference on Biometrics, ICB*, vol. Springer LNCS-3832, pp. 373–381, 2006.